Journal of Anatomy

J. Anat. (2017) doi: 10.1111/joa.12664

Congenital muscle dystrophy and diet consistency affect mouse skull shape differently

Alexander Spassov,[1,4,*] Viviana Toro-Ibacache,[2,3,*] Mirjam Krautwald,[4] Heinrich Brinkmeier[4] and Kornelius Kupczik[5]

[1]*Department of Orthodontics, University Medicine Greifswald, Greifswald, Germany*
[2]*Facultad de Odontología, Universidad de Chile, Santiago de Chile, Chile*
[3]*Department of Human Evolution, Max Planck Institute for Evolutionary Anthropology, Leipzig, Germany*
[4]*Institute of Pathophysiology, University Medicine Greifswald, Karlsburg, Germany*
[5]*Max Planck Weizmann Center for Integrative Archaeology and Anthropology, Max Planck Institute for Evolutionary Anthropology, Leipzig, Germany*

Abstract

The bones of the mammalian skull respond plastically to changes in masticatory function. However, the extent to which muscle function affects the growth and development of the skull, whose regions have different maturity patterns, remains unclear. Using muscle dissection and 3D landmark-based geometric morphometrics we investigated the effect of changes in muscle function established either before or after weaning, on skull shape and muscle mass in adult mice. We compared temporalis and masseter mass and skull shape in mice with a congenital muscle dystrophy (*mdx*) and wild type (wt) mice fed on either a hard or a soft diet. We found that dystrophy and diet have distinct effects on the morphology of the skull and the masticatory muscles. *Mdx* mice show a flattened neurocranium with a more dorsally displaced foramen magnum and an anteriorly placed mandibular condyle compared with wt mice. Compared with hard diet mice, soft diet mice had lower masseter mass and a face with more gracile features as well as labially inclined incisors, suggesting reduced bite strength. Thus, while the early-maturing neurocranium and the posterior portion of the mandible are affected by the congenital dystrophy, the late-maturing face including the anterior part of the mandible responds to dietary differences irrespective of the *mdx* mutation. Our study confirms a hierarchical, tripartite organisation of the skull (comprising neurocranium, face and mandible) with a modular division based on development and function. Moreover, we provide further experimental evidence that masticatory loading is one of the main environmental stimuli that generate craniofacial variation.

Key words: diet consistency; geometric morphometrics; *mdx* dystrophy; muscle mass; skull shape.

Introduction

The form–function relationship of the mammalian skull has been a long-lasting topic of biological research (Smith, 1993; Schwenk, 2000; De Meyer et al. 2016). The mammalian skull is formed by units or modules; i.e. traits of relative degrees of integration or shape covariation based on their developmental origin or function (Cheverud, 1982; Goswami, 2007). The skull has been largely divided into two functional regions: the structures that enclose the brain and sensory organs (cranial vault and base; referred to as the neurocranium here to match related literature), and those related to breathing and feeding, i.e. the rostrum consisting of the face and the mandible (Cheverud, 1982; Boughner et al. 2008; Drake & Klingenberg, 2010). The effect of variations in muscle loads on skull shape has been shown in animals with genetic alterations of muscle function (muscular dystrophies) or by altering diet consistency (soft vs. normal, or 'hard' food) (Kiliaridis et al. 1985; Lightfoot & German, 1998; Renaud et al. 2010; Anderson et al. 2014). Hereditary muscle dystrophies, such as congenital muscular dystrophy and x-linked dystrophies, are evident already before birth (Emery, 2002). Thus they have the potential to affect bone development from early stages of fetal development (de La

Correspondence
Alexander Spassov, Institute of Pathophysiology, University Medicine Greifswald, Greifswalder Str. 11c, 17495 Karlsburg, Germany.
T: + 49 3834 8619100; E: alexspas@uni-greifswald.de
and
Viviana Toro-Ibacache, Facultad de Odontología, Universidad de Chile, Sergio Livingstone Pohlhammer 943, Independencia, Región Metropolitana, Santiago de Chile, Chile. T: + 56 2 29781702;
E: mtoroibacache@odontologia.uchile.cl

*Equal contribution.

Accepted for publication *31 May 2017*

Porte et al. 1999; Rot-Nikcevic et al. 2006). Shifts from hard to soft food regimens alter masticatory muscle activity and can affect skull morphology during later stages (i.e. post-weaning) stages of ontogeny (see discussion in Martínez-Abadías et al. 2012). For example, it has been shown in rats and mice that a soft food diet results in a shorter and narrower face, and a shorter mandible with less pronounced bony processes as compared with their conspecifics fed on a hard diet (Kiliaridis et al. 1985; Anderson et al. 2014). These differences can be considered the result of induced postnatal changes in masticatory function. In contrast, alterations in muscle structure and function caused by genetic abnormalities, such as laminin α2-deficient dystrophies, have been associated with shorter, flattened and caudally broader skulls and shorter mandibles in mice (Lightfoot & German, 1998). Moreover, hyper-muscular mice as the result of myostatin-deficiency are brachycephalic with an anteroposteriorly elongated mandible (Vecchione et al. 2007).

The commonly used model for studying the human Duchenne muscle dystrophy is the *mdx* mouse (e.g. Spassov et al. 2010; McGreevy et al. 2015). *Mdx* mice are affected by a point mutation in the gene encoding for the cytoskeletal protein dystrophin, leading to loss of functional dystrophin in skeletal muscles (McGreevy et al. 2015). The muscles of *mdx* mice undergo fibre degeneration followed by regeneration (Turk et al. 2005), yet they are capable of reaching normal strength values during the first months of life during normal physical activity such as running (Wineinger et al. 1998) and biting (Byron et al. 2006). Histologically, *mdx* muscles are characterized by a considerable variation in fibre diameter (Spassov et al. 2010). Although most of these anomalies in *mdx* mice have been observed postnatally, muscle alterations already occur earlier in development, i.e. prenatally (de La Porte et al. 1999) and immediately after birth (Torres & Duchen, 1987). Under normal developing conditions, the effect of masticatory function has been observed acting on mouse skull shape before 35 days postnatally (shortly after weaning; Willmore et al. 2006).

The reduction of muscle function from a developmentally early stage, together with the capacity to overcome the functional deficiency under physiological demands makes *mdx* an excellent model to study skull shape changes associated with both congenital (i.e. due to a mutation) and induced (i.e. due to changes in dietary consistency) diminished muscle function. To date, only one study has looked at the effect of both factors in *mdx* mice but the analysis was limited to the mandible, using two-dimensional outline geometric morphometrics (Renaud et al. 2010). An assessment of the global effects of muscle function on muscle and skull morphology offers the possibility to better understand the functional constraints driving the development of skull shape.

Using muscle dissection, computed tomography imaging and 3D morphometrics, we assess the effect of altered muscle function on muscle mass (temporalis and masseter) and skull shape. We use a murine model of congenitally altered muscle function (*mdx* muscle dystrophy) and reduced muscle function through induced changes in dietary consistency (hard vs. soft food). Both types of altered muscle function imply reduced chewing muscle strength and lower occlusal forces, and thus less bone growth due to a low-strain environment. We predicted that an altered muscle function produced by either the muscle dystrophy and/or a soft food consistency would result in shape changes of both the cranium (i.e. neurocranium and face) and the mandible, as well as in a reduced masticatory muscle mass. In particular, we expected that the neurocranium, face and mandible were differently affected by the changes in muscle function: a soft diet would primarily affect the face and the mandible rather than the neurocranium, because the former mice reach adult form later in life and are under a higher masticatory demand (Diewert, 1985; Willmore et al. 2006).

Materials and methods

Animals and feeding regimens

Male mice of the wild type strain C57B1/10ScSn (wt, $n = 24$) and the inbred strain C57B1/10ScSn-Dmdmdx/J (*mdx*, $n = 24$) were bred at the Central Animal Facility of the University Medicine of Greifswald (Germany) and held in cages without elements for exercise. As Duchenne's syndrome is an X-linked recessive disorder, it mostly affects men and we therefore choose male mice for our study. Immediately after weaning (21–24 days of age) the wt and *mdx* groups were randomly allocated to receive either hard (normal) or soft food, resulting in four groups ($n = 12$ each) for analyses: wt hard food, wt soft food, *mdx* hard food and *mdx* soft food. The hard food consisted of common pellets and the soft food of the same pellets homogenized with water in a proportion of 1 : 2.5. Food and drinking water were provided *ad libitum* during the complete period of the experiment. All experiments were performed in accordance with the directive 2010/63/EU of the European Parliament for the protection of animals used for scientific purposes and the German animal protection act.

The death of the animals was induced at 100 ± 2 days (mean age = 100.04 days, SD = 1.03) using ether inhalation and rapid cervical dislocation. The temporalis and masseter (superficial and deep) as well as the soleus muscles were dissected and (wet) weighed. The soleus muscle was used as a control for non-masticatory-related effects, as it is typically affected and hypertrophic in *mdx* mice at this age (Pastoret & Sebille, 1995). Dissected skulls were fixed in 4.5% formalin solution and stored at 4 °C.

Computed tomography (CT) imaging

The skulls were CT scanned at the Zoological Institute and Museum of the University of Greifswald on an Xradia MicroXCT-200 system (Xradia Inc., Pleasanton, CA, USA) at 40 kV and 200 mA, with an isometric voxel size of 0.025 mm. Data reconstruction was done using specialist software (XM Controller and XM Reconstructor, v.8.1.7546, XRadia Inc.) and the resulting images were exported as TIFF files.

3D image processing and landmark placing

The image stacks were imported in AVIZO 8.0 (FEI, Hillsboro, OR, USA). Bone and teeth were segmented using a semiautomatic thresholding approach based on grey-level differences. Surface files in Polygon format (PLY) were generated and used for landmark data acquisition.

Using AVIZO, 3D landmarks were placed by the same observer (A.S.) on the PLY surface of each individual, representing a series of developmental, anatomical and biomechanically relevant structures (described in Table 1 and shown in Fig. 1). Landmark placing was done in two different sessions. The effect of measurement error was discarded via Procrustes ANOVA (Klingenberg & McIntyre, 1998), by quantifying the amount of variation caused by repeated landmark-placing relative to that caused by differences among individuals (Rosas & Bastir, 2004). Subsequently, the landmarks of the two sessions were averaged.

Landmarks were initially placed on the left and right sides and the midplane of each individual's skull. As our study focused on global shape changes, we did not specifically test for inherent yet small-scale skull asymmetries. To alleviate any potential issues, we excluded the effects of asymmetry on the results by symmetrizing the configurations; corresponding left and right landmark coordinates were reflected and then averaged. Of these generated symmetric configurations, only the landmarks on the mid-plane and the right side of the skull were used in subsequent tests, thus reducing the number of dependent variables. To ensure that skull symmetrization has no effect on overall shape changes, we performed a principal components analysis (PCA) on the matrices of shape variables representing both the original and symmetrized data. The data maintained its distribution after symmetrization (data not shown). The negligible effect of data symmetrization was then confirmed by a Mantel test on both matrices of shape data.

Statistical and shape analyses

Differences in muscle masses and skull centroid size were assessed through one-way ANOVAs and Tukey's test for pairwise comparisons and verified with non-parametric Kruskal–Wallis and Mann–Whitney tests using PAST (Hammer et al. 2001).

To study the effects of dystrophy and diet on skull shape, geometric morphometric tools were used. The landmarks of the midplane and right side underwent rotation, translation and scaling, generating Procrustes coordinates which represent the shape of each individual in subsequent analyses (Hallgrimsson et al. 2015).

Using EVAN TOOLBOX (www.evan-society.org), PCA on shape variables was first used as an exploratory analysis and also to reduce the number of dependent variables for statistical testing. Secondly, the PC scores summarizing up to 75% of the variance in the sample (PCs 1–8 in the cranium and PCs 1–6 in the mandible) were used to test between-group differences via multivariate analysis of variance (MANOVA) and verified with non-parametric MANOVA (Anderson, 2001) with 10 000 rounds of permutation using PAST. The MANOVA was also performed on the landmark configurations representing the two main parts of the cranium (i.e. neurocranium and face). All the MANOVA results were maintained when using PCs up to 90% of explained variance, but with a lower statistical power. For this reason, 75% explained variance was chosen.

As the results of this separated MANOVA supported our prediction of a differential effect of congenital and induced muscle function on the neurocranium and face, a confirmatory modularity test was performed (see Results below). The modularity test compares the degree of covariation (estimated by the RV coefficient) between the two hypothesized modules and alternative partitions (Klingenberg, 2009). Modules tend to have a low RV coefficient in comparison with alternative partitions of the same landmark configuration. Hence, a low proportion of the 100 000 alternative partitions tested showing RV coefficients lower than that of the hypothesized partition suggest an independent variation of the tested modules (Yerges et al. 2010; Jamniczky & Hallgrímsson, 2011). Landmarks defining each module are shown in Table 1. Their choice was based on definitions used in previous studies of mammal skull shape variation and modularity (Yerges et al. 2010; Jamniczky & Hallgrímsson, 2011; Anderson et al. 2014). The modularity tests were performed with MORPHOJ (Klingenberg, 2011).

The statistical power of the tests in this work was > 0.9, as assessed using G*POWER (Faul et al. 2007).

Visualization of local and general shape changes

Geometric morphometrics offers the possibility to visualize shape changes in relation to the independent variables, which is a key analysis in the present study. Surface warpings were used to depict shape differences with respect to a reference configuration (Hallgrimsson et al. 2015). The latter corresponds to the mean shape of the wt hard diet group. To this end, the PLY surface of one individual was warped to match the reference configuration, and then this reference surface was warped again to each of the group means. Warpings were scaled up (six times in the cranium and four times in the mandible, of which the latter shows more marked shape changes) to facilitate the visualization of shape changes. Surface warpings were performed in EVAN TOOLBOX.

Results

Measurement error and effect of symmetrization

Procrustes ANOVA results show that the mean squares for individual variation are significantly greater than the error for repeated landmark placing (Table 2). Hence, measurement error is negligible and does not have an effect on our subsequent results.

The Mantel test comparing shape variation in the original (left and right sides) and the symmetrized landmark configuration shows that there is a significant correlation between both data subsets (cranium: $R = 0.98$, $P < 0.01$; mandible: $R = 0.85$, $P < 0.01$). Thus, the symmetrization procedure aiming to exclude the possible nuisance of asymmetry and to reduce the number of dependent variables, does not alter the nature of shape variation in the data.

Muscle mass and skull centroid size

Masseter and soleus mass were significantly different among all four groups. In particular, masseter mass was lowest in the soft diet groups, and the soleus mass was larger in the *mdx* than in wt mice (Fig. 2, Supporting

Table 1 Landmarks used for shape analysis and centroid size calculation.

No.	Description
Cranium	
1	Most rostral end of the internasal suture (F)
2	Intersection between the nasofrontal and internasal sutures (F)
3	Intersection between the coronal and sagittal sutures (N)
4	Most caudal end of the sagittal suture (N)
5	Most caudal point of the foramen magnum and the cranium (N)
6	Point on the occipito-interparietal suture at the intersection with the straight line (from superior) connecting points 4 and 5 (N)
7	Basion (most rostral point of the foramen magnum) (N)
8	Most caudal end of the median palatine suture (F)
9	Most rostral point of the interincisive foramen (F)
10	Most vestibular and low point of the interradicular septum between incisors) (F)
11	Incisor, mesial angle (F)
12	Incisor, distal angle (F)
13	Incisor, most palatal point of the occlusal surface (F)
14	Highest point of the alveolar ridge of the incisor (F)
15	Most rostral point of the premaxilla at the opening of the nasal cavity (F)
16	Intersection between the maxilla, frontal and lacrimal bones (F)
17	Most dorsal and rostral point of the zygomatic process of the maxilla, where the lateral border of the zygomatic arch meets the infraorbital foramen (F)
18	Lateral end of the coronal suture at the temporal line (N)
19	Intersection between the squamosal, frontal and alisphenoid bones (N)
20	Dorsal end of the suture between the zygomatic process of the maxilla and the zygomatic (jugal) bone (F)
21	Ventral end of the suture between the zygomatic process of the maxilla and the zygomatic (jugal) bone (F)
22	Dorsal end of the suture between the squamosal and zygomatic (jugal) bones (F)
23	Ventral end of the suture between the squamosal and zygomatic (jugal) bones (F)
24	Most caudal point of the insertion of the deep masseter muscle. It appears as a small tubercle in the zygomatic process of the temporal (squamosal) bone (F)
25	Most caudal and ventral point at the anterior crus of the tympanic bone (N)
26	Dorsal end of the occipito-squamosal suture at the temporal line (N)
27	Most lateral point of the foramen magnum, at the caudal end of the occipital condyle (N)
28	Most lateral end of the union between the basisphenoid and occipital bones, at its ventral face (N)
29	Most lateral end of the maxillo-palatine suture (F)
30	Most distal point on the alveolar ridge of M3 (F)
31	Most caudal point of the palatine fissure (F)
32	Most mesial point on the alveolar ridge of M1 (F)
33	Most ventral point of the suture between the premaxilla and the maxilla (F)
34	Most rostral point of the palatine fissure (F)
35	Most palatal and high point on the alveolar ridge of the incisor (F)
Mandible	
1	Tip of the lower incisor
2	Lowest point on the alveolar ridge of the incisor
3	Most ventral and rostral point of the insertion area of the digastric muscle
4	Rostral end of the masseteric ridge
5	Tip of the angular process of the mandible
6	Point on the masseteric ridge perpendicularly projected from half the linear distance between points 4 and 5
7	Most caudal point of the condylar process
8	Point of the concave posterior border of the mandibular ramus, projected perpendicularly from half the linear distance between points 5 and 7
9	Most caudal point of the articular surface of the condylar process
10	Most rostral point of the articular surface of the condylar process
11	Lowest point of the mandibular notch
12	Tip of the coronoid process
13	Point at the anterior border of the coronoid process, projected perpendicularly to the rostro-caudal axis from the vestibular sulcus of M2
14	Most mesial point on the alveolar ridge of M1

(continued)

Table 1. (continued)

No.	Description
15	Most distal point on the alveolar ridge of M3
16	Most ventral point of the mental foramen
17	Most ventral point of the foramen in the pterygoid fossa
18	Most rostral and ventral point of the mandibular foramen
19	Most caudal and ventral point of the mandibular symphysis
20	Highest point of the alveolar ridge of the incisor
21	Most rostral and dorsal point of the mandibular symphysis

Hypothetical modules: N, neurocranium; F, face.

Information Table S1). After Bonferroni correction, however, the masseter mass of the wt soft diet group did not differ from that of the two hard diet groups or from the *mdx* soft diet group (Table 3). The centroid size of the cranium was significantly different among all four groups (Fig. 2, Table S1), but after Bonferroni correction, only the difference between the two extreme wt hard diet and *mdx* soft diet groups was significant (Table 3). Yet, when the neurocranium and face were analyzed separately, the centroid size of the former differed between wt and *mdx* irrespective of diet (although after Bonferroni correction, the difference between both hard diet groups and the *mdx* soft diet group was no longer statistically significant) (Fig. 2, Tables S1 and 3).

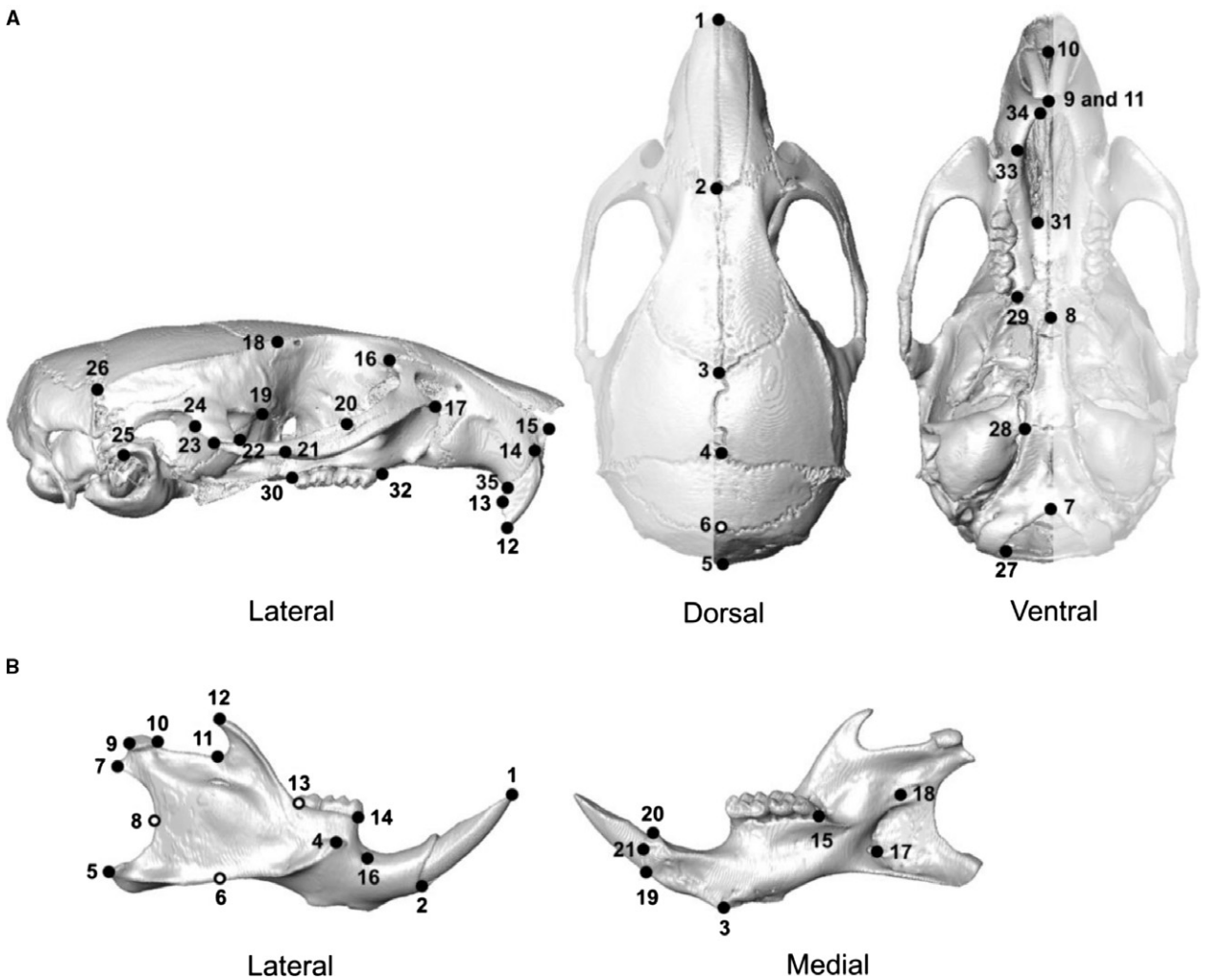

Fig. 1 Selected landmarks. Hollow landmarks represent points constructed from other landmarks. (A) Cranial landmarks, located on the right side. The left side is shown as reference. Landmark 9 in ventral view appears superimposed by landmark 11. (B) Mandibular landmarks.

Cranial and mandibular shape

Principal components analysis and MANOVA revealed that each of the four groups displayed different shapes of both the cranium and mandible (Fig. 3, Tables 4 and 5). Within the cranium, the shape of the neurocranium was significantly different between *mdx* and wt mice, without distinction between dietary groups (Tables 4 and 5). In contrast, the shape of the face and the mandible distinguished all groups from each other (Tables 4 and 5).

Shape differences among groups were found to be related to dystrophy, and those related to changes in diet consistency (red and blue arrows respectively in Fig. 4). The cranium of *mdx* mice differed from wt mainly in neurocra-

Table 2 Procrustes ANOVA for the effect of measurement error on cranial and mandibular shape.

Structure	Effect	Sum of squares	Mean squares $\times 10^7$	df	*F*	*P*-value
Cranium	Individual	0.0595	73.21	8131	8.59	< 0.01
	Repeated landmarking	0.0071	8.52	8304		
Mandible	Individual	0.0967	172.96	5593	9.18	< 0.01
	Repeated landmarking	0.0108	18.85	5712		

$N_{total} = 48$.

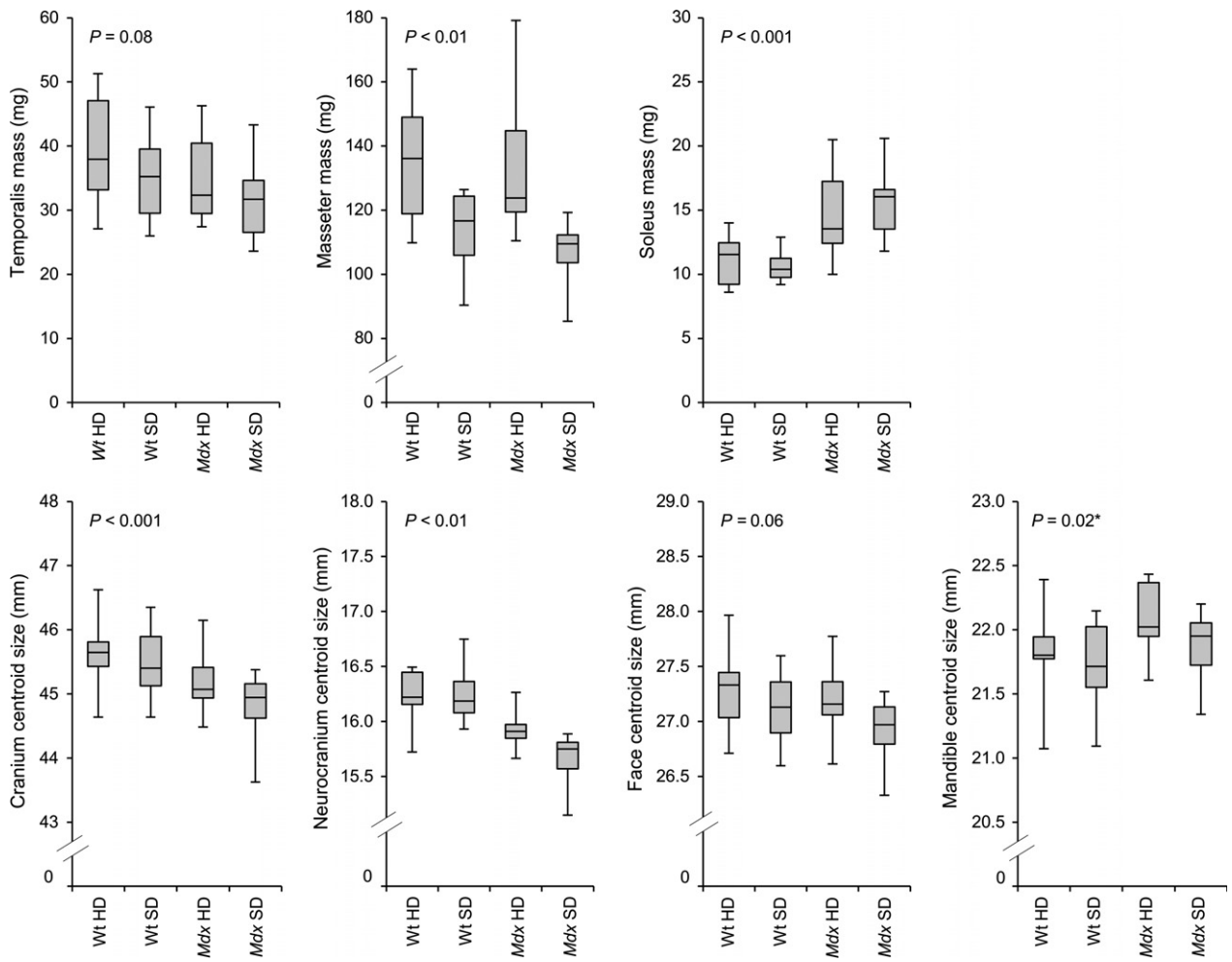

Fig. 2 Boxplot comparison of muscle mass (upper row) and centroid size (lower row) between groups. HD, hard diet, SD, soft diet. The ranges in the vertical axes have been independently adjusted to improve the visualization of data variation. The *P*-values from ANOVA are shown (statistical significance $P < 0.05$) at each plot. Values non-significant after Bonferroni correction are marked with an asterisk. The detailed results of the ANOVA are shown in Table S1.

Table 3 Tukey's pairwise group comparisons of muscle mass and centroid size (CS).

	Wt hard diet	Wt soft diet	*Mdx* hard diet	*Mdx* soft diet
Wt hard diet		Masseter mass*	Soleus mass Neurocranium CS	Masseter mass Soleus mass Cranium CS Neurocranium CS*
Wt soft diet			Soleus mass Neurocranium CS Mandible CS*	Soleus mass Cranium CS* Neurocranium CS
Mdx hard diet				Masseter mass Neurocranium CS*
Mdx soft diet				

Statistically significant differences are shown ($P < 0.05$). Non-significant values after Bonferroni correction are marked with an asterisk.

Table 4 Results of MANOVA for shape of cranium, neurocranium and face, and mandible.

Structure	Wilks' lambda	df 1	df 2	*F*	*P*-value
Cranium	0.0019	24	107.90	34.44	< 0.01
- Neurocranium*	0.0830	21	109.70	7.20	< 0.01
- Face*	0.0022	21	109.70	38.92	< 0.01
Mandible	0.0033	18	110.80	40.35	< 0.01

*Based on the scores of PCs 1–7.
P-values < 0.05 are considered statistically significant. All *P*-values < 0.01 after Bonferroni correction.

nial traits: flattened base (with respect to the palate) and vault (a and b in Fig. 4); a more dorsally placed foramen magnum and a more laterally displaced zygomatic arch with a more dorsally located rostral end (c and d in Fig. 4). In contrast, hard diet mice were distinguished from soft diet mice by facial traits: soft diet mice showed labially oriented incisors, an extended diastema and a narrow rostrum (e, f and g in Fig. 4).

In the mandible, *mdx* differed from wt mice in the vertical extension of the ramus; a more inferiorly and laterally extended masseteric positioned ridge; a relatively superior position of the digastric insertion with respect to the lower border of the ramus; and a relative less caudally extended condyle (h, i, j and k in Fig. 4). Soft diet mice exhibited a slight horizontally oriented coronoid process; a gracile alveolar process and a condyle with a small articular surface (l, m and n in Fig. 4). Similar to the face, they had a more extended diastema and labially inclined incisors (o and p in Fig. 4; Supporting Information Fig. S1). Wt hard diet mice, overall, had the most robust mandible, particularly in the mediolateral direction (Fig. 4).

The modularity test confirmed a differential effect of the congenital and induced changes in muscle function over the two main parts of the cranium (Table 6), as suggested by the MANOVA tests (Table 4). The degree of independent covariation between the neurocranium and face differed

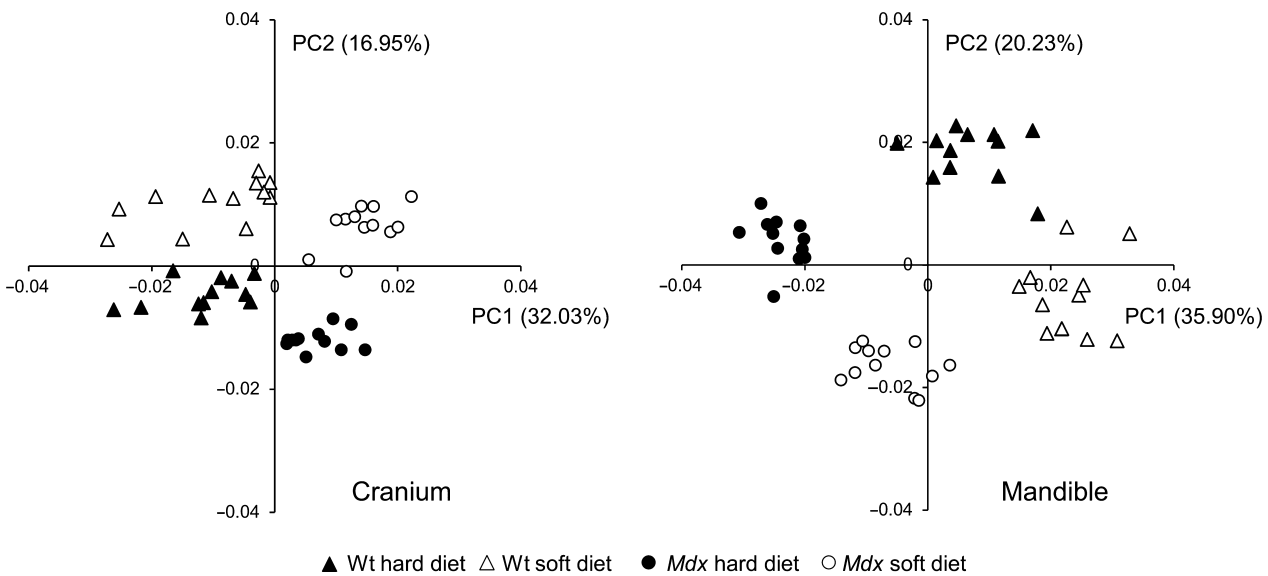

Fig. 3 Cranial and mandible shape differences. Principal components analysis of cranial and mandible shape variables; distribution of individuals ($n = 48$, 12 per group) along the first (PC1) and second (PC2) principal components, with the percentage of total variance explained by each axis shown in parentheses.

Table 5 Hotelling's pairwise group comparisons of cranium, neurocranium and face, and mandibular shape.

	Wt hard diet	Wt soft diet	*Mdx* hard diet	*Mdx* soft diet
Wt hard diet		Cranium Face Mandible	Cranium Neurocranium Face Mandible	Cranium Neurocranium Face Mandible
Wt soft diet			Cranium Neurocranium Face Mandible	Cranium Neurocranium Face Mandible
Mdx hard diet				Cranium Face Mandible
Mdx soft diet				

Statistically significant differences ($P < 0.05$) are shown. All P-values < 0.01 after Bonferroni correction.

markedly among groups. The neurocranium and face of the wt hard diet group were the most modular, followed by *mdx* hard diet and wt soft diet mice; in *mdx* soft diet mice these structures were the least modular (Table 6).

Discussion

Our study shows that the congenital (i.e. muscle dystrophy) and induced (i.e. soft food regimen) changes in muscle function have distinct effects on both the masticatory muscles and the morphology of the skull. Moreover, within the skull it has a distinctive effect on the neurocranium and the rostrum.

Mdx muscle dystrophy is known to affect skeletal muscles; however, its effect on the masticatory muscles is less well studied. Histological parameters suggest some differences in limb muscles that would make them less susceptible to damage (Muller et al. 2001; Spassov et al. 2010). A capacity of the dystrophic masticatory muscles to function under demand is suggested by our results. Specifically the masseter, which is the main jaw-closing muscle in rodents (Cox et al. 2012), was significantly larger in the hard diet groups than in the soft diet groups, irrespective of the mutation. We also observed this difference in temporalis mass, but it failed to show statistically significant differences between groups (Fig. 2, Table S1).

The marked muscle mass and skull shape differences among the four groups are helpful in understanding the differential effects of congenital vs. induced changes in masticatory function on skull shape. Furthermore, these results demonstrate a modular tendency in shaping the neurocranium vs. the rostrum, particularly in response to substantial changes in functional demands (e.g. Klingenberg, 2013). Mechanical signals such as those produced by muscle contraction are essential in bone development. They act from embryonic stages, and even low-magnitude signals induce cell differentiation and osteogenesis (Uzer et al. 2015). In *mdx* mice, although most of the tissue and muscle function anomalies were observed after 3 weeks postnatally (Turk et al. 2005), muscle alterations may already occur prenatally (de La Porte et al. 1999) and immediately after birth (Torres & Duchen, 1987). Hence, the congenital condition in *mdx* mice most likely affects the neurocranium, which reaches adult size earlier in life than the face (Leamy et al. 1999; Willmore et al. 2006). Indeed, our results show that diet consistency alone has no effect on skull size (Kiliaridis et al. 1985); yet the presence of the dystrophy does affect neurocranial size irrespective of diet.

But why does the dystrophic condition particularly affect the neurocranium? Neurocranial changes during ontogeny are strongly related to brain growth. For example, a more flexed cranial base can accommodate a larger brain, particularly in the presence of a large face (Lieberman et al. 2008). The more ventrally positioned foramen magnum in wt mice found here could therefore reflect the developmental relationship between the relative facial/neurocranial size and cranial base shape. Indeed, in our sample the neurocranium, but not the face, of *mdx* mice was smaller than that of the wt mice (Tables 3 and S1). Interestingly, a somewhat similar phenotype (flat cranial vault and medio-laterally extended zygomatic arches) to the one observed in *mdx* mice was described in adult wt mice following an acute postnatal treatment with an agonist of the hedgehog (HH) pathway (Singh et al. 2015). The HH gene family includes the Indian Hedgehog, which is involved in the ossification and shape of the cranial vault (Lenton et al. 2011). It has been shown that the *mdx* muscle dystrophy is not capable of efficiently activating the HH signalling pathway (Pinhasi et al. 2015). Hence a direct, genetically driven effect of the *mdx* mutation on bone (and thus skull) development cannot be completely ruled out and deserves further study.

Despite their different developmental origin and functional role, the bones of the neurocranium and face as well as of the neck are tightly linked anatomically and developmentally (Esteve-Altava et al. 2015). Thus, beyond the localized effects of brain growth on cranial vault formation, the potential role of facial and neck muscles on the shape of the cranial parts at both prenatal and postnatal stages also has to be considered. Among prenatal muscle-related activities in mice and rats that could be linked to neurocranial alterations are head–neck movements, mouth opening and tongue withdrawal (Narayanan et al. 1971; Suzue, 1996). Rot-Nikcevic et al. (2006) also described cervical kyphosis in amyogenic mice fetuses, and a progressive vertebral misalignment (Laws & Hoey, 2004), particularly a 'dropped head', was observed in *mdx* mice (Lefaucheur et al. 1995), which may also be linked to a more dorsally placed foramen magnum. A dropped head likely imposes functional

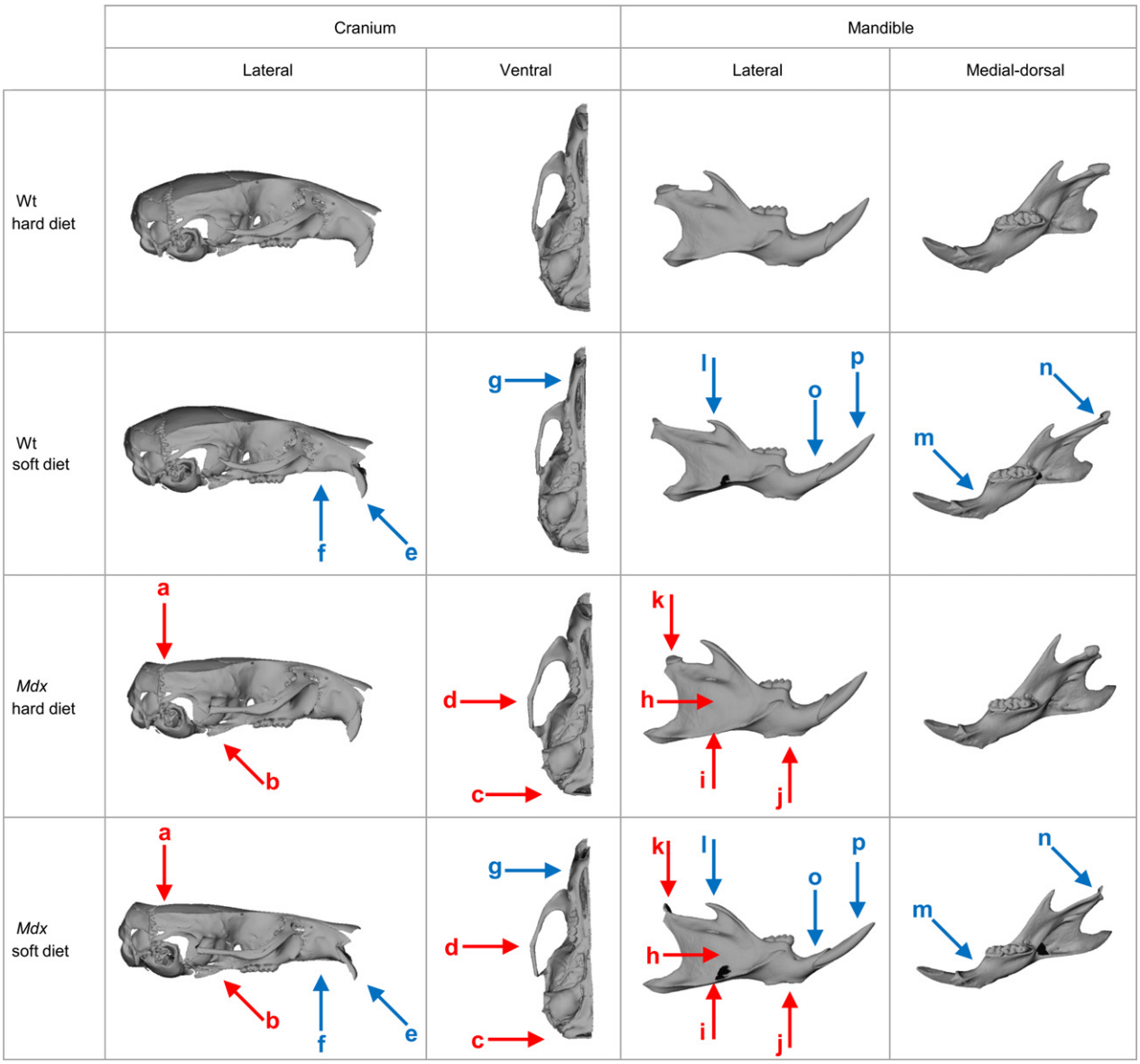

Fig. 4 Cranial and mandibular shape changes of wt soft diet, and *mdx* hard/soft diet group means with respect to the wt hard diet group mean (undeformed). Red arrows indicate changes related to muscle dystrophy, blue arrows indicate differences related to diet consistency. Specific traits are marked with lowercase letters and their detailed description is found in the main text. Warpings are magnified six times in the cranium and four times in the mandible to facilitate visualisation.

limitations. As *mdx* mice have the potential to produce muscle contraction and regenerate damaged fibres before adulthood (Turk et al. 2005), it is possible that they exert large forces with the neck–extensor muscles only to maintain a 'normal' head–neck relationship that allows for unimpeded feeding and viewing. The effect of increased dorsal neck activity on the quadrupedal mammal skull shape has not yet been dealt with in depth. However, in humans the skull–neck position has been suggested as a predictor of craniofacial development, with 'neck-extenders' showing a more vertically developed face and an increased cranial base angle (Solow & Kreiborg, 1977; Solow & Siersb, 1992; Leitao & Nanda, 2000).

The neurocranium and face are linked anatomically and functionally, yet they behave as relatively independent regions of the cranium in their development (Cheverud, 1982; Boughner et al. 2008; Drake & Klingenberg, 2010). The modularity test showed that the wt hard diet group, which can be considered the reference individuals, presents the most independent variation of both cranial parts; followed by the *mdx* hard diet and wt soft diet groups. In contrast, the *mdx* soft diet cranium is strongly integrated (Table 6). This result suggests that when there is normal muscle functioning, the independence between the neurocranium and face is maintained. It is therefore not surprising that with the loss of muscle-based functional

Table 6 Tests of modularity in the cranium of each group reporting RV coefficients and the proportion of coefficients of alternative modules that are lower than the hypothesized ones (low values indicate stronger modularity).

Structures	Group	RV coefficient	Proportion of lower RV coefficients
Neurocranium vs. face	Wt hard diet	0.67	0.05
	Wt soft diet	0.85	0.25
	Mdx hard diet	0.60	0.15
	Mdx soft diet	0.82	0.71

N_{total} = 48; 12 per group.

constraints, as in the case of the *mdx* soft diet mice, the neurocranium and face shape comparatively have a much larger degree of integration. In other words, under the lack of masticatory constraints, the face shape could be influenced by neurocranial, likely brain, development (Boughner et al. 2008).

The shape of the mandible has been shown to be highly influenced by masticatory function, and is divided in an anterior, dental portion and a posterior, muscular part (Cheverud, 2001; Anderson et al. 2014). Using different rodent species, Zelditch et al. (2009) found that the pattern and strength of covariation within the mandible is variable, and concluded that given its function as a lever, the mandible should not be decomposed into parts like the cranium because it is 'rather a single connected unit'. Moreover, it has been shown that during mastication the symphysis, alveolar region, condyle, coronoid and angular processes are under stress (Cox & Jeffery, 2015). In agreement with this conclusion, we found that, unlike in the cranium, the mutation-related and diet-related features in the mandible are spatially more overlapped, reflecting a more widespread effect of the postweaning muscle function than the effect of the dystrophy, which is less extended in time and likely of less mechanical intensity. The anterior-posterior condyle position relative to the angular process as well as the middle and lower portions of the mandibular ramus distinguished *mdx* from wt mice (Fig. 4). This result is analogous to findings in laminin-deficient mice (Vilmann et al. 1985) where the coronoid process is less affected by the mutation than are the condyle and angular process. In contrast to the conclusions of a previous study (Renaud et al. 2010), however, our data show that in *mdx* mice the mandible had an anteriorly shifted and shortened condyle rather than a posteriorly positioned and extended angular process.

Irrespective of the mutation, the shapes of the condyle, coronoid process and alveolar region distinguished hard from soft diet groups (see also Sasaguri et al. 1998; Anderson et al. 2014). These differences can be accounted for by the post-weaning growth and development of both the condyle and angular processes, which are largely dependent on the masseter (Yonemitsu et al. 2007) and lateral pterygoid muscles (Stutzmann & Petrovic, 1990). Likewise, the development of the coronoid process is known to depend upon temporalis muscle (Rot-Nikcevic et al. 2007). Indeed, here we found that the masseter as the dominant masticatory muscle in mice (Nakata, 1981) was significantly lighter in the mice fed on softened pellets than those fed on hard pellets. As muscle force depends on muscle mass, the soft food mice may have produced less masticatory loads, thus providing less mechanical stimuli to the bone (Ross et al. 2007), resulting in the observed differences in facial shape. Indeed, despite an overall weak relationship between muscle force and skull shape in humans, individuals with an orthognathic maxilla have larger temporalis muscles and thus higher muscle forces than prognathic individuals (Toro-Ibacache et al. 2016).

The effect of diet consistency on masticatory muscle mass and skull shape beyond the presence of muscle dystrophy was also reflected by the labially inclined incisors and the more extended diastemata in the maxilla and mandible of the two soft food groups (Fig. 4). These differences can also be seen in the unscaled renderings of the original specimens (Fig. S1) and is in agreement with Kiliaridis et al. (1985) and Anderson et al. (2014). This configuration suggests an increased outlever arm for biting on the incisors, effectively reducing bite strength (Samuels, 2009). In fact, as was shown by Anderson et al. (2014), hard food eaters had a higher mechanical advantage (i.e. the inlever/outlever moment arms ratio) than soft food eaters. This is supported by preliminary observations in our sample that the soft diet mice had posteriorly more extended mandibular incisors, with the curve of upper incisors in a slightly more horizontal position compared with the mice fed with normal pellets (Fig. S1). It is likely that the incisors were worn down less and at a slower rate in the soft food mice and that the consequent lack in mechanical signal led to an overgrowth at the cervical loop of the incisor roots below the molars (see Klein et al. 2008).

In conclusion, our results confirm the prediction that diminished masticatory function, as the result of a genetic mutation and an induced dietary shift, resulted in changes in masticatory muscle mass and skull shape. Within the skull, shape differences were spatially well defined due to its modular nature. Within the cranium, the neurocranium was largely affected by the genetic condition and the face, as well as most of the mandible and masseter mass, by diet consistency. It is conceivable that the differential response of the neurocranium and face is possibly linked to differences in the onset of altered muscle activity and pattern and timing of bone development. Although, so far, bone alterations in *mdx* mice can be explained by loading-induced modelling (Schipilow et al. 2013), other effects related to the *mdx* mutation that eventually affect bone developmental pathways cannot be completely ruled out

and require further study. The functional plasticity of the masticatory muscles and the skull, particularly of the face and mandible, may facilitate dystrophic mice in adopting a normal facial morphology under a hard diet regimen. Our study confirms a hierarchical, tripartite organization of the skull with a modular division of the skull (into neurocranium, face and mandible) based on developmental and functional constraints, as has been suggested by several studies dealing with craniofacial integration in mammals in general and specifically in humans. In particular, one of the main environmental drivers of human facial variation is said to be masticatory loading in response to variations in food consistency. Our study clearly supports this notion.

Acknowledgements

We are very grateful to Ingrid Pieper for technical assistance in the mouse feeding experiments. We would also like to thank Gabriele Uhl for use of the microCT scanner in her care and Jakob Krüger for CT scanning the skulls. We are also grateful to Stefan Schlager, Germán Manríquez Soto and Jens van den Brandt as well as the Editor and two reviewers whose comments helped to improve this manuscript. Parts of this study are based on ideas originally conceived by Dragan Pavlovic, to whom we are grateful.

Author contributions

A.S., H.B., V.T.I. and K.K. designed the study. M.K. collected muscle data. A.S. collected the landmark data; A.S. and V.T.I. analyzed the muscle and landmark data. All authors wrote the article.

Funding

This research was in part supported by the Max Planck Society (Germany) and Comisión Nacional de Investigación Científica y Tecnológica (FONDECYT Grant 11150175, Chile).

References

Anderson MJ (2001) A new method for non-parametric multivariate analysis of variance. *Austral Ecol* **26**, 32–46.

Anderson P, Renaud S, Rayfield E (2014) Adaptive plasticity in the mouse mandible. *BMC Evol Biol* **14**, 85.

Boughner JC, Wat S, Diewert VM, et al. (2008) Short-faced mice and developmental interactions between the brain and the face. *J Anat* **213**, 646–662.

Byron CD, Hamrick MW, Wingard CJ (2006) Alterations of temporalis muscle contractile force and histological content from the myostatin and *Mdx* deficient mouse. *Arch Oral Biol* **51**, 396–405.

Cheverud JM (1982) Phenotypic, genetic, and environmental morphological integration in the cranium. *Evolution* **36**, 499–516.

Cheverud JM (2001) The genetic architecture of pleiotropic relations and differential epistasis. In: *The Character Concept in Evolutionary Biology* (ed. Wagner GP), pp. 411. San Diego: Academic Press.

Cox PG, Jeffery N (2015) The muscles of mastication in rodents and the function of the medial pterygoid. In: *Evolution of the Rodents: Advances in Phylogeny, Functional Morphology and Development* (eds Cox PG, Hautier L). Cambridge: Cambridge University Press.

Cox PG, Rayfield EJ, Fagan MJ, et al. (2012) Functional evolution of the feeding system in rodents. *PLoS One* **7**, e36299.

De Meyer J, Christiaens J, Adriaens D (2016) Diet-induced phenotypic plasticity in European eel (*Anguilla anguilla*). *J Exp Biol* **219**, 354–363.

Diewert VM (1985) Development of human craniofacial morphology during the late embryonic and early fetal periods. *Am J Orthod* **88**, 64–76.

Drake AG, Klingenberg CP (2010) Large scale diversification of skull shape in domestic dogs: disparity and modularity. *Am Nat* **175**, 289–301.

Emery AEH (2002) The muscular dystrophies. *Lancet* **359**, 687–695.

Esteve-Altava B, Diogo R, Smith C, et al. (2015) Anatomical networks reveal the musculoskeletal modularity of the human head. *Sci Rep* **5**, 8298.

Faul F, Erdfelder E, Lang A-G, et al. (2007) G*Power 3: a flexible statistical power analysis program for the social, behavioral, and biomedical sciences. *Behav Res Methods* **39**, 175–191.

Goswami A (2007) Cranial modularity and sequence heterochrony in mammals. *Evol Dev* **9**, 290–298.

Hallgrimsson B, Percival CJ, Green R, et al. (2015) Morphometrics, 3D imaging, and craniofacial development. In: *Current Topics in Developmental Biology* (ed. Yang C), pp. 561–597, Waltham, Massachussetts: Academic Press.

Hammer Ø, Harper D, Ryan P (2001) PAST: paleontological statistics software package for education and data analysis. *Paleontol Electron* **4**, 9.

Jamniczky HA, Hallgrímsson B (2011) Modularity in the skull and cranial vasculature of laboratory mice: implications for the evolution of complex phenotypes. *Evol Dev* **13**, 28–37.

Kiliaridis S, Engström C, Thilander B (1985) The relationship between masticatory function and craniofacial morphology. I. A cephalometric longitudinal analysis in the growing rat fed a soft diet. *Eur J Orthod* **7**, 273–283.

Klein OD, Lyons DB, Balooch G, et al. (2008) An FGF signaling loop sustains the generation of differentiated progeny from stem cells in mouse incisors. *Development* **135**, 377–385.

Klingenberg CP (2009) Morphometric integration and modularity in configurations of landmarks: tools for evaluating a priori hypotheses. *Evol Dev* **11**, 405–421.

Klingenberg CP (2011) MorphoJ: an integrated software package for geometric morphometrics. *Mol Ecol Resour* **11**, 353–357.

Klingenberg CP (2013) Cranial integration and modularity: insights into evolution and development from morphometric data. *Hystrix* **24**, 16.

Klingenberg CP, McIntyre GS (1998) Geometric morphometrics of developmental instability: analyzing patterns of fluctuating asymmetry with Procrustes methods. *Evolution* **52**, 1363–1375.

de La Porte S, Morin S, Koenig J (1999) Characteristics of skeletal muscle in *mdx* mutant mice. *Int Rev Cytol* **191**, 99–148.

Laws N, Hoey A (2004) Progression of kyphosis in *mdx* mice. *J Appl Physiol* **97**, 1970–1977.

Leamy LJ, Routman EJ, Cheverud JM (1999) Quantitative trait loci for early- and late-developing skull characters in mice: a

test of the genetic independence model of morphological integration. *Am Nat* **153**, 201–214.

Lefaucheur JP, Pastoret C, Sebille A (1995) Phenotype of dystrophinopathy in old *mdx* mice. *Anat Rec* **242**, 70–76.

Leitao P, Nanda RS (2000) Relationship of natural head position to craniofacial morphology. *Am J Orthod Dentofac Orthop* **117**, 406–417.

Lenton K, James AW, Manu A, et al. (2011) Indian hedgehog positively regulates calvarial ossification and modulates bone morphogenetic protein signaling. *Genesis* **49**, 784–796.

Lieberman DE, Hallgrímsson B, Liu W, et al. (2008) Spatial packing, cranial base angulation, and craniofacial shape variation in the mammalian skull: testing a new model using mice. *J Anat* **212**, 720–735.

Lightfoot PS, German RZ (1998) The effects of muscular dystrophy on craniofacial growth in mice: a study of heterochrony and ontogenetic allometry. *J Morphol* **235**, 1–16.

Martínez-Abadías N, Esparza M, Sjøvold T, et al. (2012) Pervasive genetic integration directs the evolution of human skull shape. *Evolution* **66**, 1010–1023.

McGreevy JW, Hakim CH, McIntosh MA, et al. (2015) Animal models of Duchenne muscular dystrophy: from basic mechanisms to gene therapy. *Dis Models Mech* **8**, 195–213.

Muller J, Vayssiere N, Royuela M, et al. (2001) Comparative evolution of muscular dystrophy in diaphragm, gastrocnemius and masseter muscles from old male *mdx* mice. *J Muscle Res Cell Motil* **22**, 133–139.

Nakata S (1981) Relationship between the development and growth of cranial bones and masticatory muscles in postnatal mice. *J Dent Res* **60**, 1440–1450.

Narayanan CH, Fox MW, Hamburger V (1971) Prenatal development of spontaneous and evoked activity in the rat (*Rattus norvegicus albinus*). *Behaviour* **40**, 100–133.

Pastoret C, Sebille A (1995) *Mdx* mice show progressive weakness and muscle deterioration with age. *J Neurol Sci* **129**, 97–105.

Pinhasi R, Eshed V, von Cramon-Taubadel N (2015) Incongruity between affinity patterns based on mandibular and lower dental dimensions following the transition to agriculture in the near east, Anatolia and Europe. *PLoS One* **10**, e0117301.

Renaud S, Auffray J-C, de la Porte S (2010) Epigenetic effects on the mouse mandible: common features and discrepancies in remodeling due to muscular dystrophy and response to food consistency. *BMC Evol Biol* **10**, 28.

Rosas A, Bastir M (2004) Geometric morphometric analysis of allometric variation in the mandibular morphology of the hominids of Atapuerca, Sima de los Huesos site. *Anat Rec A Discov Mol Cell Evol Biol* **278A**, 551–560.

Ross CF, Dharia R, Herring SW, et al. (2007) Modulation of mandibular loading and bite force in mammals during mastication. *J Exp Biol* **210**, 1046–1063.

Rot-Nikcevic I, Reddy T, Downing K, et al. (2006) $Myf5^{-/-}$: $MyoD^{-/-}$ amyogenic fetuses reveal the importance of early contraction and static loading by striated muscle in mouse skeletogenesis. *Dev Genes Evol* **216**, 1–9.

Rot-Nikcevic I, Downing K, Hall B, et al. (2007) Development of the mouse mandibles and clavicles in the absence of skeletal myogenesis. *Histol Histopathol* **22**, 51–60.

Samuels JX (2009) Cranial morphology and dietary habits of rodents. *Zool J Linn Soc* **156**, 864–888.

Sasaguri K, Jiang H, Chen J (1998) The effect of altered functional forces on the expression of bone-matrix proteins in developing mouse mandibular condyle. *Arch Oral Biol* **43**, 83–92.

Schipilow JD, Macdonald HM, Liphardt AM, et al. (2013) Bone micro-architecture, estimated bone strength, and the muscle-bone interaction in elite athletes: an HR-pQCT study. *Bone* **56**, 281–289.

Schwenk K (2000) *Feeding: Form, Function And Evolution in Tetrapod Vertebrates*. San Diego: Academic Press.

Singh N, Dutka T, Devenney BM, et al. (2015) Acute upregulation of hedgehog signaling in mice causes differential effects on cranial morphology. *Dis Models Mech* **8**, 271–279.

Smith KK (1993) The form of the feeding apparatus in terrestrial vertebrates: studies of adaptation and constraint. In: *The Skull* (eds Hanken J, Hall BK), pp. 150–196. Chicago: The University of Chicago Press.

Solow B, Kreiborg S (1977) Soft-tissue stretching: a possible control factor in craniofacial morphogenesis. *Eur J Oral Sci* **85**, 505–507.

Solow B, Siersb S (1992) Cervical and craniocervical posture as predictors of craniofacial growth. *Am J Orthod Dentofac Orthop* **101**, 449–458.

Spassov A, Gredes T, Gedrange T, et al. (2010) Histological changes in masticatory muscles of *mdx* mice. *Arch Oral Biol* **55**, 318–324.

Stutzmann JJ, Petrovic AG (1990) Role of the lateral pterygoid muscle and meniscotemporomandibular frenum in spontaneous growth of the mandible and in growth stimulated by the postural hyperpropulsor. *Am J Orthod Dentofac Orthop* **97**, 381–392.

Suzue T (1996) Movements of mouse fetuses in early stages of neural development studied in vitro. *Neurosci Lett* **218**, 131–134.

Toro-Ibacache V, Zapata Muñoz V, O'Higgins P (2016) The relationship between skull morphology, masticatory muscle force and cranial skeletal deformation during biting. *Ann Anat* **203**, 59–68.

Torres LFB, Duchen LW (1987) The mutant *mdx*: inherited myopathy in the mouse. Morphological studies of nerves, muscles and end-plates. *Brain* **110**, 269–299.

Turk R, Sterrenburg E, de Meijer E, et al. (2005) Muscle regeneration in dystrophin-deficient *mdx* mice studied by gene expression profiling. *BMC Genom* **6**, 98.

Uzer G, Thompson WR, Sen B, et al. (2015) Cell mechanosensitivity to extremely low magnitude signals is enabled by a LINCed nucleus. *Stem Cells* **33**, 2063–2076.

Vecchione L, Byron C, Cooper GM, et al. (2007) Craniofacial morphology in myostatin-deficient mice. *J Dent Res* **86**, 1068–1072.

Vilmann H, Juhl M, Kirkeby S (1985) Bone-muscle interactions in the muscular dystrophic mouse. *Eur J Orthod* **7**, 185–192.

Willmore KE, Leamy L, Hallgrímsson B (2006) Effects of developmental and functional interactions on mouse cranial variability through late ontogeny. *Evol Dev* **8**, 550–567.

Wineinger MA, Abresch RT, Walsh SA, et al. (1998) Effects of ageing and voluntary exercise on the function of dystrophic muscle form from *mdx* mice. *Am J Phys Med Rehabil* **77**, 20–27.

Yerges LM, Klei L, Cauley JA, et al. (2010) Candidate gene analysis of femoral neck trabecular and cortical volumetric bone mineral density in older men. *J Bone Miner Res* **25**, 330–338.

Yonemitsu I, Muramoto T, Soma K (2007) The influence of masseter activity on rat mandibular growth. *Arch Oral Biol* **52**, 487–493.

Zelditch M, Wood A, Swiderski D (2009) Building developmental integration into functional systems: function-induced integration of mandibular shape. *Evol Biol* **36**, 71–87.

Supporting Information

Additional Supporting Information may be found in the online version of this article:

Table S1. Muscle mass and centroid size (CS) comparisons between groups.

Fig. S1. 3D renderings of mouse skulls showing the enamel lining of the incisors and the enamel caps of the molars in four representative wt/*mdx* and hard/soft food animals, respectively. The red lines indicate the course of the upper (solid) and lower incisors (dotted) in the wt soft, *mdx* hard and *mdx* soft diet mice relative to the incisor morphology in the wt hard diet mouse. Note the differences in inclination in the maxillary incisors and the length of the mandibular incisors relative to the molars between the hard food and soft food mice.